Biosensors and Bioelectronics 25 (2010) 1301–1306

Contents lists available at ScienceDirect

Biosensors and Bioelectronics

journal homepage: www.elsevier.com/locate/bios

Ionic-liquid/NH_2-MWCNTs as a highly sensitive nano-composite for catalase direct electrochemistry

Parvaneh Rahimi[a], Hossain-Ali Rafiee-Pour[b], Hedayatollah Ghourchian[b,*], Parviz Norouzi[a], Mohammad Reza Ganjali[a]

[a] Center of Excellence in Electrochemistry, Faculty of Chemistry, University of Tehran, P.O. Box 14155-6455, Tehran, Iran
[b] Laboratory of Microanalysis, Institute of Biochemistry and Biophysics, University of Tehran, Enghelab Street, Tehran, Iran

ARTICLE INFO

Article history:
Received 8 September 2009
Received in revised form 8 October 2009
Accepted 14 October 2009
Available online 23 October 2009

Keywords:
Catalase
Room temperature ionic-liquid
Amine functionalized multi-walled carbon nanotubes
Direct electron transfer

ABSTRACT

A nano-composite material consisting of amine functionalized multi-walled carbon nanotubes and a room temperature ionic-liquid (1-butyl-3-methylimidazolium tetrafluoroborate) was prepared and used to construct a novel catalase (Ct) based biosensor for the determination of hydrogen peroxide. The modified electrode exhibited a quasi-reversible cyclic voltammogram corresponding to the Fe(II)/Fe(III) redox couple in the heme prosthetic group of Ct with a formal potential of −460 mV in 0.1 M phosphate buffer solution at pH 7.0. The nano-composite film showed an obvious promotion of the direct electron transfer between Ct and the underlying electrode. The apparent charge transfer rate constant and transfer coefficient for electron transfer between the electrode surface and enzyme were calculated as 2.23 s^{-1} and 0.45, respectively. The immobilized Ct exhibited a relatively high sensitivity (4.9 nA/nM) toward hydrogen peroxide. Under the optimized experimental conditions, hydrogen peroxide was detected in the concentration range from 8.6 to 140 nM with a detection limit of 3.7 nM at S/N = 3. The modified electrode was stable for two weeks with no observable change in the cyclic voltammograms.

1. Introduction

Design and development of third-generation biosensors based on metalloenzymes have mainly been indebted to bioelectrochemistry (Santucci et al., 1994; Jiang et al., 2008). In addition, the direct electrochemistry of proteins can provide a model for mechanistic studies of their electron transfer activity in the biological systems (Zhou et al., 2008). Unfortunately, direct electron transfer between enzyme and the naked electrode surface is usually difficult due to the large spatial separation between the enzyme prosthetic group and the electrode surface. However, incorporating the redox enzymes into a special conductive film on electrode surfaces facilitates the electron transfer of the redox enzymes (Hong et al., 2006; Mogharrab et al., 2007). But, further investigation to find new methods for extolling protein electron transfer efficiency is required.

Room temperature ionic-liquids (RTILs) are stable salts, composed of an organic cation and an organic/inorganic anion, and are preserved in the liquid state over a wide temperature range. They have unusual properties such as high chemical and thermal stabilities, relatively high ionic conductivity, non-flammability, negligible vapor pressure and wide electrochemical windows (Buzzeo et al., 2004; Zhao et al., 2004). In addition, unlike organic solvents of comparable polarity, RTILs maintain the bioactivity of enzyme and improve its selectivity and reaction rate (Park and Kazlauskas, 2003). The RTILs can be mainly applied to biocatalytic reactions based on two aspects. Firstly, they can be used as a supporting electrolyte for promoting the direct electron transfer of protein to the electrode. A number of studies have shown that biosensors can be operated in RTILs instead of aqueous medium, resulting in a prolonged life time of the biosensor (Xiong et al., 2007; Wang et al., 2007a,b). Secondly, RTILs can easily be used as an electrode modifier for sensor development (Dai et al., 2009). Modifying the electrode surface with an ionic-liquid thin film and then immobilizing the enzyme of choice on that film was also shown to be useful in preparing biosensors for several applications (Du et al., 2007; Zhao et al., 2007; Sun et al., 2007).

Carbon nanotubes (CNTs) as a type of highly conductive nanomaterials have been reviewed by Wang (2005). CNTs have been examined for their excellent electrocatalytic abilities and antifouling properties and, thus, can be used in electrochemical biosensors. They promote electron transfer rate when used as an electrode material in electrochemical reactions (Wan et al., 2009). Recently, researchers developed biosensors with high sensitivity and good biocompatibility using a mixture of CNTs and RTILs. To modify the surface of a glassy carbon or graphite electrode using RTIL/CNTs nano-composites, one way is dispersing RTIL/CNTs or RTIL/CNT/polymer in a suitable solvent and applying the mixture to

* Corresponding author. Tel.: +98 21 66408920; fax: +98 21 66404680.
E-mail address: hadi@ibb.ut.ac.ir (H. Ghourchian).

0956-5663/$ – see front matter © 2009 Elsevier B.V. All rights reserved.
doi:10.1016/j.bios.2009.10.020

electrode modification (Wang et al., 2007; Xiao et al., 2007; Liu et al., 2007; Zhao et al., 2005). Preparation of RTIL/CNT paste electrodes by direct mixing of nanotubes with a suitable RTIL (either in solid or in liquid form at room temperature) is another method for preparing the CNT modified electrode (Torabi Kachoosangi et al., 2009). The third way is depositing multi-walled CNTs (MWCNTs) suspension on GC electrode and immersing the modified electrode in RTIL and protein solution respectively (Xiang et al., 2008). This method has several merits including low process temperature, molecular resolution of composition, thickness control and a wide variety of appropriate building blocks (Hu et al., 2008).

In this report, we examined the ability of a composite consisting of a typical RTIL and NH_2 functionalized MWCNTs to act as a modifier to achieve the direct electron transfer of catalase (Ct). The Ionic-liquid/NH_2-MWCNTs nano-composite could effectively facilitate the direct electron transfer of Ct to the electrode therefore it was applied to developing a biosensor for H_2O_2 detection.

2. Materials and methods

2.1. Chemicals

Ct (EC 1.11.1.6, from bovine liver, 2100 units/mg) was purchased from Sigma (Saint Louis, MO, USA) and used without further purification. 1-Butyl-3-methylimidazolium tetrafluoroborate ([BMIM]BF_4), as a typical RTIL, was purchased from Sigma. Multi-wall carbon nanotubes (MWCNTs), prepared by chemical vapor deposition, were purchased from Shenzhen Nanotech Port Ltd. Co. (China). Potassium dihydrogen phosphate (KH_2PO_4), dipotassium hydrogen phosphate (K_2HPO_4) and ethylenediamine ($C_2H_4[NH_2]_2$) were obtained from Merck. All solutions were prepared in double-distilled deionized water. Hydrogen peroxide (H_2O_2) stock solutions were prepared by appropriate dilutions of 30% (v/v) H_2O_2 in deionized water. Thionyl chloride ($SOCl_2$) was purchased from Acros Organics. All other chemicals were of analytical grade and used without further purification.

2.2. MWCNTs functionalization

MWCNTs were functionalized according to the literature (Jeong et al., 2006) as follow: At first, purified MWCNTs were treated with concentrated HNO_3 in order to introduce carboxyl groups on their surface. Next, 20 mg of these MWCNTs was dispersed in 1 mL of $SOCl_2$ by sonication for 5 min. The mixture was refluxed for 24 h at 50–70 °C, filtered, and washed with deionized water to remove any unreacted $SOCl_2$. An amine group was attached to the MWCNTs by stirring the filtrate in 5 mL of ethylenediamine for 5 days at 50–70 °C and filtered again. The residue was washed with anhydrous ethyl alcohol to remove any excess ethylenediamine (Lee and Yoo, 2005). The NH_2-MWCNTs obtained were dried under vacuum at room temperature.

2.3. Apparatus and measurements

Electrochemical studies were carried out using an electrochemical system (EG&G model 263A potentiostat/galvanostat) controlled by a PowerSuite software package and a GPIB interface. All electrochemical studies were performed using a conventional three-electrode cell at 25 ± 1 °C. A working modified glassy carbon (GC) electrode (bare or modified with nano-composites film) (from Azar Electrode, Uromia, Iran), a saturated silver/silver chloride (Ag/AgCl) (3 M KCl solution) reference electrode (from Metrohm), and a platinum wire counter electrode was used. All potentials were measured and reported vs. the Ag/AgCl reference electrode. Fourier transform infrared spectra were recorded using a Fourier transform infrared (FTIR) spectrometer (Model Nexus 870, Thermo Nicolet Co. USA). Scanning electron microscopic (SEM) images were obtained using a SEM Model LEO 440i, UK.

2.4. Electrode preparation

For electrode preparation, 1 mg of NH_2-MWCNTs was dispersed in 1 mL of dimethylformamide using an ultrasonic bath to give a black suspension. The GC (3 mm in diameter) electrode was polished carefully with 0.3 and 0.05 μm alumina slurry, and sonicated in water and ethanol, respectively. The cleaned GC electrode was treated by dropping 2.5 μL of NH_2-MWCNTs suspension and then dried in air. The prepared NH_2-MWCNTs/GC electrode was immersed in pure [BMIM]BF_4 solution and left for 10 h at 4 °C to adsorb a layer of RTIL on electrode surface (the modified electrode was denoted as RTIL/NH_2-MWCNTs/GC). Finally, the modified electrode was immersed in Ct solution (10 mg/mL, pH 7.0, PBS) for 10 h at 4 °C. During this process Ct was immobilized on the surface of RTIL-nanohybrid film and the Ct/RTIL/NH_2-MWCNTs/GC biosensor was assembled.

3. Results and discussion

3.1. FTIR characterization of functionalized MWCNTs

Fig. 1A shows the FTIR spectra for pristine MWCNTs (dashed line) and NH_2 functionalized MWCNTs (solid line). At pristine MWCNTs, a weak peak at 1630 cm^{-1} was assigned to C–C stretching. However after functionalization, FTIR spectrum shows a new peak at ~1570 cm^{-1} (due to the in-plane N–H molecular vibrations of the amine group), two peaks at 2860 and 2940 cm^{-1} and one peak at 2357 cm^{-1} due to the vibrations of C–H and C–O bonds, respectively. These indicate existence of new functional groups upon functionalization process. The peak at 3440 cm^{-1} corresponded to O–H stretching.

3.2. Morphology

Fig. 1B and C shows SEM images of NH_2-MWCNTs/GC and Ct/RTIL/NH_2-MWCNTs/GC modified electrode respectively. It can be seen that NH_2-MWCNTs exist as bundles, which are entangled with one another (Fig. 1B). It is clear in Fig. 1C that the thickness of NH_2-MWCNTs was increased by addition of Ct/RTIL. This indicates that the Ct/RTIL has been successfully deposited onto NH_2-MWCNTs surface.

3.3. Direct electrochemistry of Ct

The direct electrochemistry of Ct has already been reported by Salimi et al. (2005, 2007) and Hashemnia et al. (2009). In the present work, a highly sensitive nano-composite consists of RTIL and NH_2-MWCNTs, was used to efficiently immobilize Ct on a GC electrode and preserving its activity. At pH 7.0, Ct is negatively charged and therefore, the anionic functional groups of Ct may show affinity to both the NH_2 groups of MWCNTs and the positively charged imidazolium ions of RTIL.

Fig. 2 shows the cyclic voltammograms of different electrodes in 0.1 M phosphate buffer solution, pH 7.0 (PBS) at a scan rate of 0.1 V s^{-1}. The enzyme on GC electrode (Ct/GC) showed no electrochemical redox peak in the potential range studied (Curve a). It is well known that the heme prosthetic group of Ct is deeply embedded in a protective protein shell, which makes the direct electron communication with electrodes extremely difficult. Also the NH_2-MWCNT/GC electrode did not show any response because it contains no electroactive species (Curve b). However, regarding the role of CNTs in mediating the electron transfer between Ct and

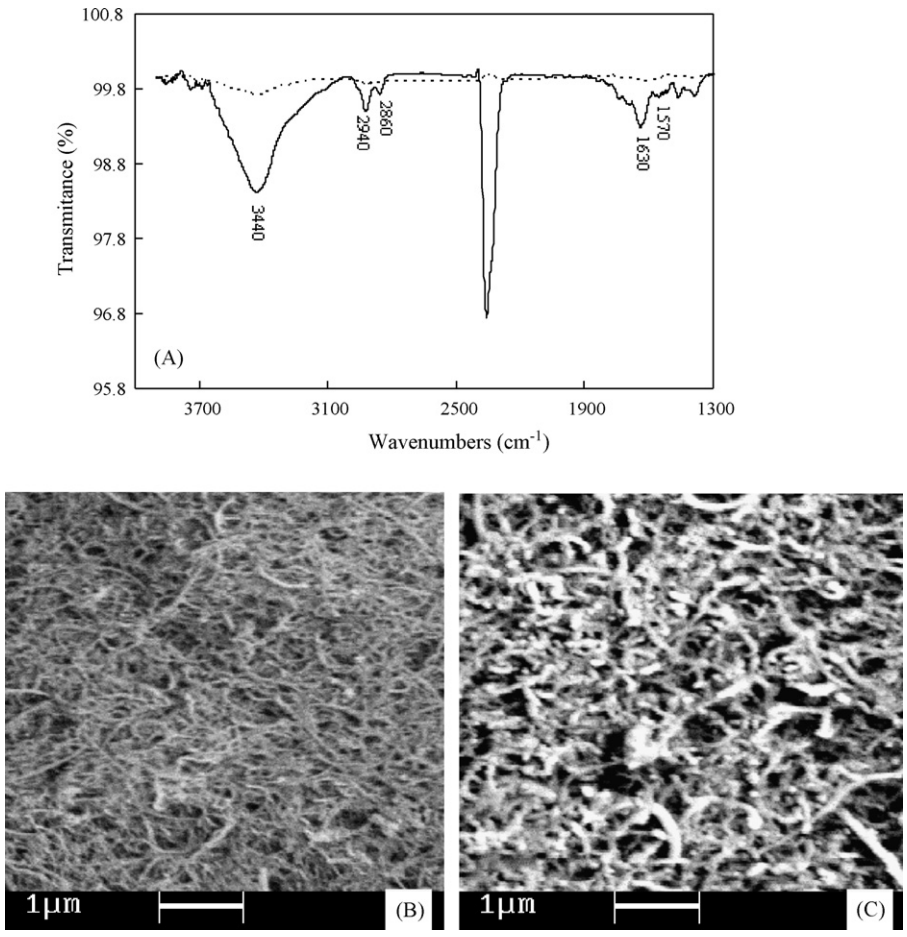

Fig. 1. FTIR spectra of pristine MWCNTs (dashed line) and NH_2 functionalized MWCNTs (solid line) (A) and SEM images of NH_2-MWCNTs/GCE (B) and Ct/RTIL/NH_2-MWCNTs/GCE (C).

the electrode surface (Prakash et al., 2009), when Ct was immobilized on the NH_2-MWCNTs/GC electrode, it showed a couple of small and broad redox peaks (Curve c). These peaks are related to the Fe(III)/Fe(II) redox couple of heme prosthetic group of Ct. Curve d, as a control, was obtained by the RTIL/NH_2-MWCNTs/GC in the same condition. But, as indicated by Curve e, immobilization of Ct on the RTIL/NH_2-MWCNTs/GC showed a pair of well-defined and nearly symmetric redox anodic and cathodic peaks (respectively at −427 and −492 mV vs. Ag/AgCl). As explained by Zhao et al. (2005),

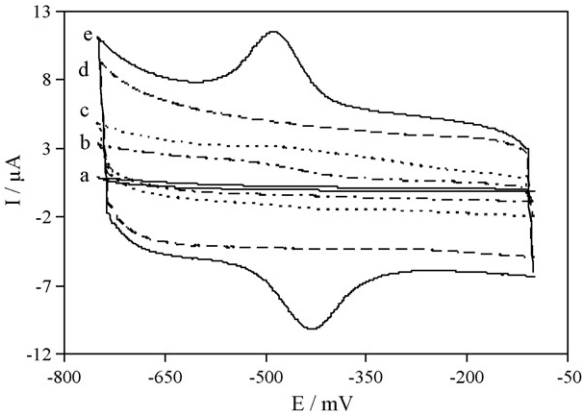

Fig. 2. Cyclic voltammograms of different modified electrodes: (a) Ct/GC, (b) NH_2-MWCNTs/GC, (c) Ct/NH_2-MWCNTs/GC, (d) RTIL/NH_2-MWCNTs/GC and (e) Ct/RTIL/NH_2-MWCNTs/GC. The results were obtained in 0.1 M phosphate buffer solution, pH 7.0, at the scan rate of 0.1 V s^{-1}.

RTIL might interact with MWCNTs through π–π, π–cationic and/or hydrophobic–hydrophobic interactions. In addition, according to Wei et al. (2009), protein can bind to RTIL through ionic interaction. Therefore, RTIL on the surface of NH_2-MWCNTs plays a crucial role in Ct immobilization. In such a condition the RTIL/NH_2-MWCNTs nano-composite could establish an intimate relation between Ct molecules and the glassy carbon electrode surface and so, a relatively easy electronic communication between the enzyme and the modified electrode was founded. The ratio of the cathodic/anodic current was found to be close to 1, and the potential difference between the two peak currents, ΔE_p, was measured as 65 mV, which is close to Nernst potential.

The formal potential ($E^{\circ\prime}$) for Ct of −0.460 V (vs. Ag/AgCl) was calculated by taking the average of the cathodic and anodic peak potential. This value is consistent with −476 mV reported for heme prosthetic group of Ct (Jiang et al., 2008).

Fig. 3A shows the cyclic voltammograms of Ct/RTIL/NH_2-MWCNTs/GC electrode in PBS at different scan rates. The plots of anodic and cathodic peak currents of Ct as a function of potential scan rate are shown in Fig. 3B, indicating a typical surface-controlled electrochemical process as expected for immobilized systems.

The peak-to-peak separation, at scan rates below 300 mV s^{-1}, was found to be approximately 60 mV. In addition, the formal potential is almost independent of the potential scan rate indicating a facile charge transfer kinetic over the range of applied sweep rate. But at scan rates above 750 mV s^{-1}, the peak separations begin to increase, indicating the limitation arising from charge transfer kinetics (Fig. 3C).

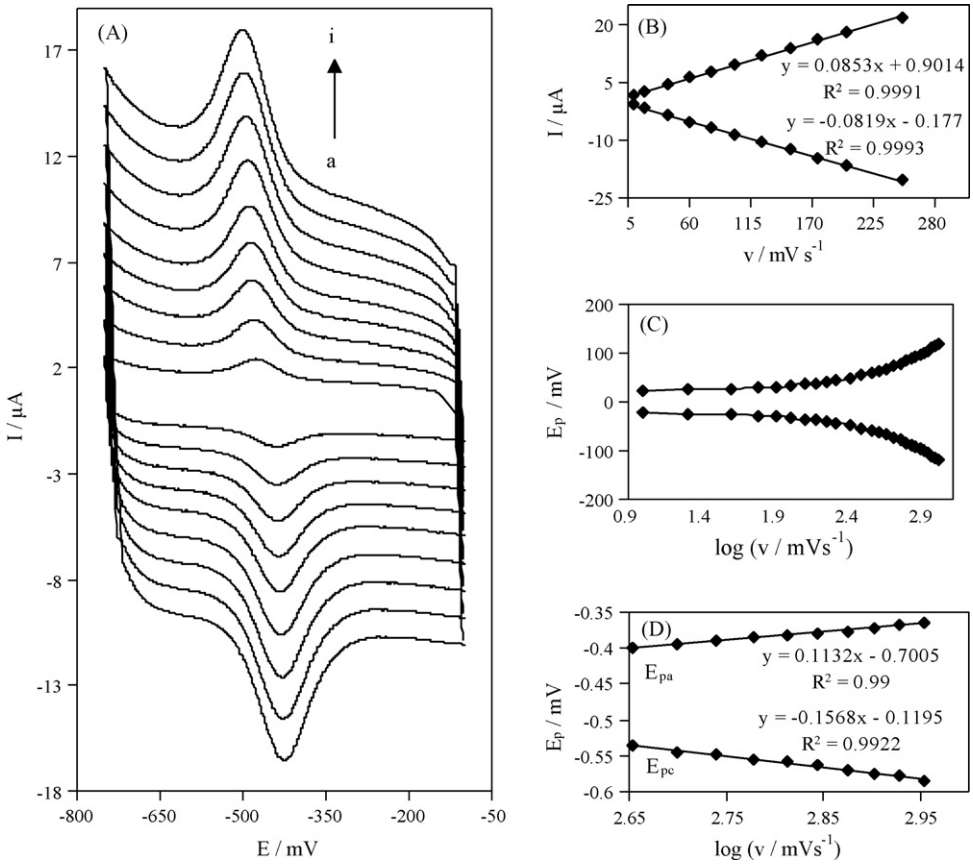

Fig. 3. (A) Cyclic voltammograms of Ct/RTIL/NH_2-MWCNTs/GCE in 0.1 M phosphate buffer solution, pH 7.0 at various scan rates of 20, 40, 60, 80, 100, 125, 150, 175 and 200 mV s^{-1} from a to i respectively; (B) plot of I_p vs. υ; (C) plot of E_p vs. log υ; (D) plot of E_{pa} and E_{pc} vs. log υ.

The kinetic parameters of α and k_s can be calculated using Laviron's model (Laviron, 1979). When the concentration of surface-confined electroactive species is smaller than one and ΔE_p ($E_{pa} - E_{pc}$) > 200/n mV, the general expressions for the linear sweep voltammetric response, are indicated by Eqs. (1)–(3):

$$E_{pc} = E^{\circ} + \frac{RT}{\alpha_c nF} \ln\left[\frac{\alpha_c}{m}\right] \quad (1)$$

$$E_{pa} = E^{\circ} + \frac{RT}{\alpha_a nF} \ln\left[\frac{\alpha_a}{m}\right] \quad (2)$$

$$\log k_s = \alpha \log(1-\alpha) + (1-\alpha)\log\alpha - \log\left(\frac{RT}{nF\nu}\right) - \alpha(1-\alpha)\frac{nF\Delta E_p}{2.3RT} \quad (3)$$

where, $m = (RT/F)(k_s/n\nu)$, k_s is the apparent charge transfer rate constant, α is the charge transfer coefficient, n is the number of electron transferred in the rate-determining reaction, ΔE_p is the peak potential seperation; R, T, and F have their usual meanings (R = 8.314 J mol^{-1} K^{-1}, T = 298 K, F = 96483 C mol^{-1}) and ν is the scan rate. α can be calculated using the plot of peak potentials (E_p) vs. logarithm of scan rate (log ν). As seen in Fig. 3C, the plot of $E_p = f(\log \nu)$ yields two straight lines with slopes equal to $-2.3RT/\alpha_c nF$ and $2.3RT/\alpha_a nF$ for the cathodic and anodic peaks, respectively. It was observed in Fig. 3D that for scan rates above 750 mV s^{-1} the values of E_p (defined as $E_{pc\,(or\,pa)} - E^{\circ\prime}$) were proportional to log ν. Thus, using the slopes of mentioned plots and based on Eqs. (1) and (2), the values for $\alpha_c n$ and $\alpha_a n$ were calculated to be 0.38 and 0.52, respectively, with the average value of 0.45 for αn. Therefore, the values for n and α could be estimated as 1 and 0.45, respectively, with the latter within the reported range of 0.3 and 0.7 (Ma et al., 2000). From the values of ΔE_p (for sweep rates > 750 mV s^{-1}) and based on Eq. (3), an average value of k_s was obtained to be 2.23 ± 0.08 s^{-1}. For a reversible surface reaction, the peak current has been given by Eq. (4) (Wang, 1999):

$$I_p = \frac{n^2F^2\nu A\Gamma_c}{4RT} \quad (4)$$

the surface concentration of electroactive species (Γ_c) can be estimated from the slope of peak currents vs. scan rate plot (Fig. 3B). Where, ν is the sweep rate, A is the surface area (0.0314 cm^2) of the modified electrode, and the other symbols have their usual meanings. From the slope of cathodic peak currents vs. scan rate, the calculated surface concentration of Ct is 2.88×10^{-10} mol cm^{-2}, suggesting an approximate monolayer of Ct on the surface of RTIL/NH_2-MWCNTs/GC electrode, which is comparable to 2.4×10^{-10} mol cm^{-2} reported previously (Prakash et al., 2009).

Long-term stability is one of the most important properties for biosensors and bioreactors. The operational stability of the Ct/RTIL/NH_2-MWCNTs/GC electrode was investigated by cyclic voltammetry. About 93% of the peak height of Ct on the nanocomposite layer retained after 90 cycles at the scan rate of 100 mV s^{-1} while the peak potential remained unchanged. To control storage stability, electrodes were stored in PBS at 4 °C for two weeks and there was no observable change in the cyclic voltammograms. It seems that the high stability of biosensor is mainly due to the ionic microenvironment produced by the RTIL/NH_2-MWCNTs nano-composite and strong adsorption of Ct into the nano-composite.

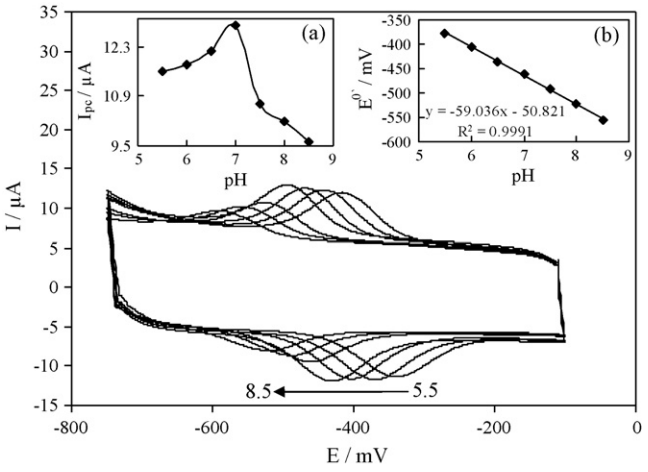

Fig. 4. Cyclic voltammograms of Ct/RTIL/NH_2-MWCNTs/GCE in 0.1 M phosphate buffer solution at pH 5.5, 6.0, 6.5, 7.0, 7.5, 8.0 and 8.5 from right to left respectively. Insets a and b show the plot of I_{pc} vs. pH and E° vs. pH respectively.

3.4. Effect of pH on the peak potential

The voltammetric behavior of the Ct/RTIL/NH_2-MWCNTs/GC electrode was characterized at various pH by CV. Fig. 4 shows peak currents of the electrode in PBS at various pH ranging from 5.5 to 8.5. As seen in Fig. 4, inset a, the cathodic peak current rose with pH change from 5.5 to 7, then it decreased when the pH was increased from 7 to 8.5. The maximum cathodic current was obtained at pH 7, therefore it was chosen as the optimal pH for next experiments. This optimum pH value of 7 is in agreement with that reported for Ct by Jiang et al. (2008). As illustrated in Fig. 4 (inset b) the formal potential ($E^{\circ\prime}$) of the surface redox couple was pH dependent. The results showed that the slope ($E^{\circ\prime}$/pH) is 59.03 mV/pH over a pH range from 5.5 to 8.5. This slope was close to the Nernstian value of 59.2 mV for a one-electron, one-proton process (Bond, 1980).

3.5. Biocatalytic activity of biosensor

Preliminary experiments for elucidation of the biocatalytic activity of the Ct/RTIL/NH_2-MWCNTs/GC electrode toward H_2O_2 were performed using cyclic voltammetry in the potential range from −0.1 to −0.75 V (vs. Ag/AgCl). Fig. 5 shows typical cyclic voltammograms of Ct at modified electrode in the presence of different concentrations of H_2O_2. With increasing the concentration of H_2O_2, the reduction peak current increased, while the oxidation peak current decreased, showing electrocatalytic reduction process of H_2O_2.

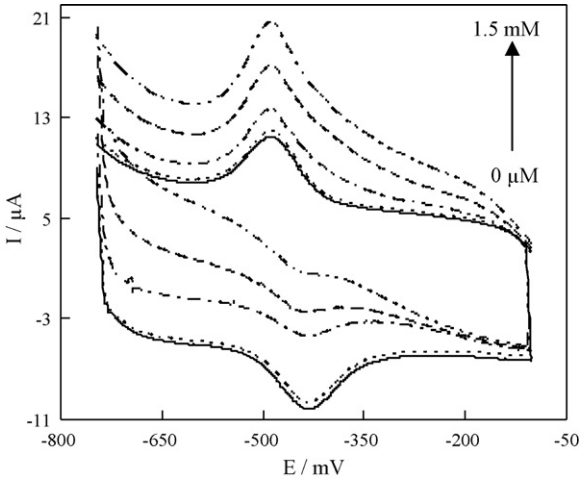

Fig. 5. Cyclic voltammograms of Ct/RTIL/NH_2-MWCNTs/GCE in 0.1 M phosphate buffer solution of pH 7.0 containing (from inner to outer) 0, 0.1, 400, 900 and 1500 μM H_2O_2 at a scan rate of 0.1 V s^{-1}.

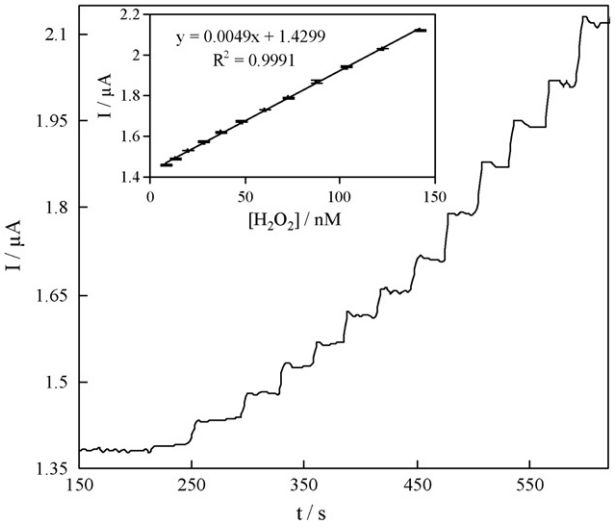

Fig. 6. Amperometric response of Ct/RTIL/NH_2-MWCNTs/GCE to hydrogen peroxide. The electrode was held at −0.55 V (vs. Ag/AgCl) while its rotation speed was 500 rpm in 0.1 M phosphate buffer solution, pH 7.0. The final concentration of H_2O_2 after each successive addition was 8.6, 13.5, 19.9, 27.9, 37.2, 47.9, 59.9, 72.9, 87.1, 103.4, 121.8 and 141.9 nM, respectively. Inset shows the calibration plot for H_2O_2 determination.

3.6. Amperometric response of biosensor to H_2O_2

The typical amperometric responses of the Ct/RTIL/NH_2-MWCNTs/GC electrode at a detection potential of −550 mV (vs. Ag/AgCl) toward H_2O_2 is shown in Fig. 6. The inset shows a calibration plot based on reduction current responses in the presence of H_2O_2. By denoting the amperometric response as the time needed to reach the steady state current, this was estimated to be 6 s. The biosensor response toward H_2O_2 concentration is linear from 8.6 to 140 nM. The linear equation is represented by: $I(\mu A) = 0.0049C(nM) + 1.4299$ ($n = 12$) with a correlation coefficient of 0.9991. Based on signal to noise ratio (S/N) of 3, the detection limit is estimated to be 3.7 nM with a relatively high sensitivity of 4.9 nA/nM. The detection limit and the sensitivity are much superior than those obtained by Ct/SWNT-CHI (2.5 μM, 6.32 μA mM^{-1}, CHI: chitosan) (Jiang et al., 2008), Ct/NiO (10 μM, 1.92 μA mM^{-1}) (Salimi et al., 2007), Ct/MWCNT (1 μM, 3.3 nA μM^{-1}) (Salimi et al., 2005), and Ct/MC (0.44 μA μM^{-1}, MC: methyl cellulose) (Li et al., 2004). The relative standard deviation of the biosensor response to 8.6 nM H_2O_2 was 3.3% for three successive measurements.

For the immobilized Ct, the relationship between the catalytic current and the concentration of substrate followed the Michaelis–Menten kinetic mechanism. The apparent Michaelis–Menten constant (K_m^{ap}), which gives an indication of the enzyme–substrate kinetics, can be obtained from the Lineweaver–Burk equation (Kamin and Wilson, 1980).

$$\frac{1}{I_{ss}} = \frac{1}{I_{max}} + \frac{K_m^{ap}}{I_{max}C} \quad (5)$$

The K_m^{ap} and maximum current (I_{max}) values of the H_2O_2 sensor were determined by the analysis of the slope and the intercept of the Lineweaver–Burk plot of $1/I$ vs. $1/C$. According to this plot, the K_m^{ap} and I_{max} were calculated to be 118 nM and 3.9 μA, respectively. The obtained K_m^{ap} value is much smaller than

those reported for Ct immobilized on single-wall carbon nanotubes film (11.8 mM) (Jiang et al., 2008), MWCNTs film (1.7 mM) (Salimi et al., 2005), silica sol–gel and cysteine modified gold electrode (50 μM) (Di et al., 2006) and nickel oxide nano-scale islands (0.96 mM) (Salimi et al., 2007). The small value of K_m^{ap} indicates the high affinity of immobilized Ct to H_2O_2. This indicates not only the feasibility of nano-composite in mediating a relatively easy electronic communication between enzyme and modified electrode, but also prepares a sufficient microenvironment for enzyme–substrate interaction. Therefore, the biosensor displayed much better electrochemical characteristics such as higher sensitivity and much lower detection limit than those reported previously.

4. Conclusion

The immobilized Ct on the modified electrode exhibits a direct and quasi-reversible electrochemical reaction. This can be attributed to an excellent microenvironment that RTIL/NH_2-MWCNT nano-composite provides to Ct. Meanwhile, the ionic-liquid assembled on the NH_2-MWCNTs further accelerates the electron transfer between Ct and the electrode. Simultaneously, the positively charged RTIL provided extra interaction between NH_2-MWCNTs and Ct, which is helpful for the immobilization of Ct. Characteristics such as quasi-reversible cyclic voltammograms (peak current ratio of 0.98), small value of K_m^{ap}, high sensitivity, long-term stability, and much lower detection limit relative to the data reported in the literature, all indicate that the nano-composite could not only establish a relatively easy electronic communication between enzyme and the modified electrode but also prepare a suitable microenvironment for enzyme–substrate interaction.

Acknowledgments

Financial supports provided by the Research Council of the University of Tehran and Iran National Science Foundation (INSF) are gratefully appreciated.

References

Bond, A.M., 1980. Modern Polarographic Methods in Analytical Chemistry [M]. Marcle Dekkes Inc., New York, pp. 27–45.
Buzzeo, M.C., Hardacre, C., Compton, R.G., 2004. Anal. Chem. 76, 4583–4588.
Dai, Z., Xiao, Y., Yu, X., Mai, Z., Zhao, X., Zou, X., 2009. Biosens. Bioelectron. 24, 1629–1634.
Di, J., Zhang, M., Yao, K., Bi, S., 2006. Biosens. Bioelectron. 22, 247–252.
Du, P., Liu, S., Wu, P., Cai, C., 2007. Electrochim. Acta 52, 6534–6547.
Hashemnia, S., Ghourchian, H., Moosavi-Movahedi, A.A., Faridnouri, H., 2009. J. Appl. Electrochem. 39, 7–14.
Hong, J., Ghourchian, H., Moosavi-Movahedi, A.A., 2006. Electrochem. Commun. 8, 1572–1576.
Hu, S., Lu, Q., Xu, Y., 2008. Electrochemical Sensors, Biosensors and Their Biomedical Applications, p. 564.
Jeong, J.S., Jeon, S.Y., Lee, T.Y., Park, J.H., Shin, J.H., Alegaonkar, P.S., Berdinsky, A.S., Yoo, J.B., 2006. Diamond Relat. Mater. 15, 1839–1843.
Jiang, H.J., Yang, H., Akins, D.L., 2008. J. Electroanal. Chem. 623, 181–186.
Kamin, R.A., Wilson, G.S., 1980. Anal. Chem. 52 (8), 1198–1205.
Laviron, E., 1979. J. Electroanal. Chem. 101, 19–28.
Lee, T.Y., Yoo, J.B., 2005. Diamond Relat. Mater. 14, 1888–1890.
Li, Y.M., Chen, X.T., Li, J., Liu, H.H., 2004. Electrochim. Acta 9, 3195–3200.
Liu, Y., Huang, L., Dong, S., 2007. Biosens. Bioelectron. 23, 35–41.
Ma, H., Hu, N., Rusling, J., 2000. Langmuir 16, 4969–4975.
Mogharrab, N., Ghourchian, H., Amininasab, M., 2007. Biophys. J. 92, 1192–1203.
Park, S., Kazlauskas, R.J., 2003. Curr. Opin. Biotechnol. 14, 432–437.
Prakash, P.A., Yogeswaran, U., Chen, S.M., 2009. Sensors 9, 1821–1844.
Salimi, A., Noorbakhsh, A., Ghadermarz, M., 2005. Anal. Biochem. 344, 16–24.
Salimi, A., Noorbakhsh, A., Ghadermarzi, M., 2007. Sens. Actuators B 123, 530–537.
Santucci, R., Picciau, A., Campanella, L., Brunori, M., 1994. Curr. Top. Electrochem. 3, 313–328.
Sun, W., Gao, R., Jiao, K., 2007. J. Phys. Chem. B 111, 4560–4567.
Torabi Kachoosangi, R., Musameh, M.M., Abu-Yousef, I., Yousef, J.M., Kanan, S.M., Xiao, L., Davies, S.G., Russell, A., Compton, R.G., 2009. Anal. Chem. 81, 435–442.
Wan, J., Bi, J., Du, P., Zhang, S., 2009. Anal. Biochem. 386, 256–261.
Wang, J., 1999. Analytical Electrochemistry. VCH, New York, p. 38.
Wang, J., 2005. Electroanalysis 17, 7–14.
Wang, Q., Tang, H., Xie, Q., Tan, L., Zhang, Y., Li, B., Yao, S., 2007. Electrochim. Acta 52, 6630–6637.
Wang, S., Chen, T., Zhang, Z., Pang, D., 2007a. Electrochem. Commun. 9, 1337–1342.
Wang, S., Xiong, H., Zeng, Q., 2007b. Electrochem. Commun. 9, 807–812.
Wei, W., Jin, H.H., Zhao, G.C., 2009. Microchim. Acta 164, 167–171.
Xiang, C., Zou, Y., Sun, L.X., Xu, F., 2008. Electrochem. Commun. 10, 38–41.
Xiao, F., Zhao, F., Li, J., Yan, R., Yu, J., Zeng, B., 2007. Anal. Chim. Acta 596, 79–85.
Xiong, H., Chen, T., Zhang, X., Wang, S., 2007. Electrochem. Commun. 9, 1648–1654.
Zhao, F., Wu, X., Wang, M., Liu, Y., Gao, L., Dong, S., 2004. Anal. Chem. 76, 4960–4967.
Zhao, G., Xu, M., Ma, J., Wei, X., 2007. Electrochem. Commun. 9, 920–924.
Zhao, Q., Zhan, D., Ma, H., Zhang, M., Zhao, Y., Jing, P., Zhu, Z., Wan, X., Shao, Y., Zhuang, Q., 2005. Front. Biosci. 10, 326–334.
Zhou, H., Lu, T.H., Shi, H.X., Dai, Z.H., Huang, X.H., 2008. J. Electroanal. Chem. 612, 173–178.